Rheology and Molecular Weight Distribution of Hyperbranched Polymers

Suneel,* D. M. A. Buzza, D. J. Groves, and T. C. B. McLeish

IRC in polymer Science and Technology, Department of Physics and Astronomy, University of Leeds, Leeds LS2 9JT, U.K.

D. Parker, A. J. Keeney, and W. J. Feast

IRC in Polymer Science and Technology, Department of Chemistry, University of Durham, Durham DH1 3LE, U.K.

Received May 28, 2002

ABSTRACT: We study the melt rheology and molecular weight distribution of four short chain branched hyperbranched polyesters with different molecular weights and containing branched monomers of various alkyl chain lengths n ($2 \rightarrow 4$; n is the number of CH_2 groups in the alkyl chain). We find that the molecular weight distribution for all our samples obeys the static scaling form $n(M) \sim M^{-\tau}\exp(-M/M_{\mathrm{char}})$ where $n(M)$ is the number density of hyperbranched polymers with mass M, M_{char} is the largest characteristic molecular weight, and τ is the polydispersity exponent. The values of τ for all our samples (either 1.35 or 1.55) are close to but not the same as the mean field value of $\tau = 1.5$, a consequence of the fact that our polymers were synthesized under non-mean-field polycondensation conditions. For all our samples, we found that the rheology at low and intermediate frequencies could be modeled accurately using a dynamic scaling theory based on the Rouse model. This confirms that these hyperbranched polymers behave as polymeric fractals which are essentially unentangled. For these polymers, the fractal dimension in the melt was found to be consistent with the hyperscaling relation for hyperbranched polymers $d_f = 3$, although we found rheology to be rather insensitive to d_f for our system.

1. Introduction

There has been considerable interest recently in hyperbranched polymers which are highly branched tree like molecules prepared by a one-pot condensation[1,2] of AB_x type monomers ($x \geq 2$). The simplified one step synthesis gives rise to very polydisperse systems with high molecular weights in contrast to dendrimers produced by a more complicated process, which have very low polydispersity and relatively low molecular weights. The properties of hyperbranched polymers lie between those of dendrimers and linear polymers and in some cases mimic, at least qualitatively, the unusual properties of dendrimers, for example, the nonmonotonic variation of the intrinsic viscosity with molecular weight.[3] However the lower cost of synthesizing hyperbranched polymers makes them commercially more viable than dendrimers. Hyperbranched polymers find potential applications in drug delivery, coatings and as rheology modifiers for processing;[4−7] this serves as a strong driving force for studying the rheology of these novel materials.

Most melt rheological studies on hyperbranched polymers[8−14] focus on long-chain branched systems or intermediate-chain branched systems which are entangled or close to the onset of entanglement. The presence of entanglements considerably complicates the analysis of the rheological data for these highly branched systems. In this paper, we focus on short-chain branched systems which are unentangled. (We define long-, intermediate-, and short-chain branch, respectively, as where the molecular weight between branch points is much greater than, comparable to, and much less than the entanglement molecular weight.) In fact, it is a nontrivial statement that hyperbranched polymers with short-chain branching and high molecular weight are unentangled. This is because while it is clear that entanglements will not occur at the level of spacers between branch points (owing to the short spacer length), it is not clear that entanglements do not occur on longer length-scales, for example, between larger dendritic units. We shall delay further discussion of this subtle point to section 2 of this paper.

There have been comparatively fewer rheological studies on short chain branched dendritic systems (i.e., either dendrimers or hyperbranched polymers). Existing studies[15−17] use dendritic polymers of relatively low molecular weight. The low molecular weights of these systems means that the distinctive contribution of the dendritic architecture to the frequency-dependent rheology is very limited; for example the viscoelasticity due to the dendritic molecular architecture has too narrow a frequency range or has frequencies which are too high to be analyzed by conventional rheometers. In contrast, this study involves polydisperse, high molecular weight hyperbranched polymers, where the viscoelasticity due to the dendritic molecular architecture has a broad frequency range and easily lies within the frequency window of conventional rheometry. This allows us to characterize important features about the fractal nature of the branched molecules using rheology (specifically the fractal dimension d_f). The specific polymers used in our study are hyperbranched aromatic polyesters synthesized from the polycondensation of a series of dimethyl 5-(ω-hydroxyalkoxy)isophthalates (Figure 1), that is AB_2 monomers. Branched monomers of various alkyl chain lengths n ($2 \rightarrow 4$; n is the number of CH_2 groups in the alkyl chain) were used; this allowed us to study the effect of the monomer local structure on rheology. Different extents of reaction were also used; this allowed

10.1021/ma020820r CCC: $22.00
Published on Web 11/08/2002

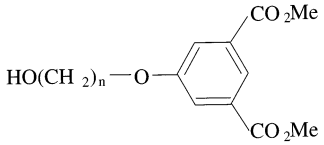

Figure 1. Structure of 5-(hydroxyalkoxy)isopthalate.

us to study the effect of molecular weight and polydispersity on rheology.

The rest of this paper is organized as follows. In section 2, we outline the theoretical models used to analyze the molecular weight distribution and rheology of the hyperbranched polymers. In section 3, we outline the experimental details of our study. Section 4 constitutes the meat of the paper, where we present experimental results for size exclusion chromatography (SEC) and rheology, analyze the data using the theoretical models in section 2, and discuss our results. Section 5 is our conclusion.

2. Theory

2.1. Static Scaling. Flory showed that the polycondensation of AB_x type monomers can never form an infinite network, that is, a gel.[18,19] However when the fraction of reacted A groups $p_A \rightarrow 1$ (or the fraction of reacted B groups $p_B \rightarrow 1/x$), the average molecular weight becomes large and we shall assume that on large enough length (or mass) scales, the hyperbranched polymers are fractal objects, so that the mass of any part of the polymer m scales with its size r according to $m \sim r^{d_f}$; here d_f is the fractal dimension. For convenience, we shall describe the hyperbranched polymers in terms of polymers on a fully occupied lattice. Flory derived $n(N)$ (the number of hyperbranched polymers with degree of polymerization N per lattice site) for the condensation polymerization of AB_x using the "tree-approximation" (i.e., mean-field theory)[18,19] which neglects excluded volume interactions and the possibility of intramolecular loops forming. More recently, $n(N)$ has also been calculated to the same level of approximation by Müller et al.[20] and Yan et al.[21−23] In the limit $p_A \rightarrow 1$, one can show that the mean-field result for $n(N)$ obeys the static scaling form

$$n(N) = N^{-\tau} f(N/N_{\text{char}}) \tag{1}$$

where $f(N/N_{\text{char}})$ is an (exponential) cutoff function that cuts off the power law scaling at large mass scales N_{char}, where $N_{\text{char}} \sim (1 - p_A)^{-1/\sigma}$ is the largest characteristic degree of polymerization in the system. In mean-field theory, $\tau = {}^3/_2$, $\sigma = {}^1/_2$ and $f(N/N_{\text{char}}) \sim \exp[-N/N_{\text{char}}]$. For our hyperbranched polymers, the spacer length between branch points N_x is short ($N_x \approx 2$), so that we are not in the mean-field regime of the polycondensation (e.g., it is known that loops are present in these systems[24]). However, as we shall see in subsection 4.1, the scaling form given by eq 1 works well for our system, though the value of τ and the form of the cutoff function will in general be different from those predicted by mean-field theory. This situation is analogous to polymer gelation where eq 1 is obeyed in both the mean-field and critical regimes, though τ and $f(N/N_{\text{char}})$ are different in the two regimes.[25] In practice, we find that a simple exponential form for the cutoff function works well for the molecular weight distribution of our system as well.

For the dynamic scaling model for hyperbranched polymers which we present in the next subsection, we shall use two different forms for the cutoff function. The first is the simple exponential function mentioned above, that is

$$f(N/N_x, N/N_{\text{char}}) = \begin{cases} \dfrac{N_{\text{char}}^{\tau-2}}{\Gamma(2-\tau,a)} \exp\left(-\dfrac{N}{N_{\text{char}}}\right) & \text{for } N > N_x \\ 0 & \text{for } N < N_x \end{cases} \tag{2}$$

where $a = N_x/N_{\text{char}}$ and $\Gamma(a, z) = \int_z^\infty t^{a-1}e^{-t}\,dt$ is the incomplete Γ function.

The second is an even simpler double step function,

$$f(N/N_x, N/N_{\text{char}}) = \begin{cases} \dfrac{(\tau-2)N_x^{\tau-2}}{1-(N_x/N_{\text{char}})^{\tau-2}} & \text{for } N_x < N < N_{\text{char}} \\ 0 & \text{for } N < N_x \text{ or } N > N_{\text{char}} \end{cases} \tag{3}$$

Note that $f(N/N_x, N/N_{\text{char}})$ cuts off the power-law distribution at small mass scales N_x (the spacer length between branch points) as well as at large mass scales N_{char}. The prefactor in front of the exponential in eq 2 and the constant value for f for $N_x < N < N_{\text{char}}$ in eq 3 have been determined from the normalization condition $\int n(N)N\,dN = 1$.

A number of measurable quantities are ratios of moments of the molecular weight distribution given by eq 1

$$N_q = \frac{\int n(N)N^q\,dN}{\int n(N)N^{q-1}\,dN} \tag{4}$$

For example, $q = 2$, 3 yields the weight-average degree of polymerization N_w and z-average degree of polymerization N_z respectively. One can easily show that for $2 < \tau < 3$ (e.g., polymer gels), $N_q \propto N_{\text{char}}$ for $q \geq 3$ while for $1 < \tau < 2$ (e.g., hyperbranched polymers), $N_q \propto N_{\text{char}}$ for $q \geq 2$. This means that for $2 < \tau < 3$, the lowest order moment ratio that is proportional to N_{char} is N_z while for $1 < \tau < 2$, the lowest order moment ratio that is proportional to N_{char} is N_w.

In systems belonging to the percolation universality class (e.g., polymer gels within the Ginzburg zone), $\tau > 2$ and the fractal dimension d_f is related to the exponent τ and the dimension of space d via the hyperscaling relation $d_f = d/(\tau - 1)$ (for $z \leq d \leq 6$). Our preliminary analysis shows that hyperbranched polymers do not belong to the percolation universality class. This leads to hyperbranched polymers obeying a modified hyperscaling relation within the Ginzburg zone, which is given by (see Appendix)

$$d_f = d \ (d \leq 4) \tag{5}$$

that is, d_f is independent of τ (the Ginzburg zone is the regime where mean-field theory breaks-down). Note that since the spacer length between branch points in our system is short ($N_x \approx 2$), the polycondensation of our hyperbranched polymers almost certainly occurs within the Ginzburg zone. We therefore expect the fractal dimension for our hyperbranched polymers in the

melt to obey eq 5. Hyperscaling implies that a given polymer chain is only strongly overlapped with smaller ones.[26] As we shall see in the next subsection, this may have important implications for the dynamics of hyperbranched polymers.

2.2. Dynamic Scaling. To model the dynamic shear viscoelasticity of our hyperbranched polymers, we use the dynamic scaling model of Rubinstein et al.[27] This assumes a Rouse model for the polymer chains, that is, where hydrodynamic interactions are screened and the polymer chains are unentangled. The latter assumption is in fact nontrivial because while it is clear that entanglements do not occur at the level of spacers between branch points for our hyperbranched polymers (owing to the short spacer length), it is not clear that entanglements do not occur on longer length-scales, for example, between larger dendritic units. Some justification for assuming that the polymer chains are unentangled comes from the hyperscaling relation eq 5. As mentioned earlier, hyperscaling implies that a given polymer is only strongly overlapped with smaller ones; it is therefore not unreasonable to assume that, on the time scale of relaxation of larger molecules, the smaller ones have completely relaxed and are therefore no longer effective in forming entanglements with the larger chains. By assuming that hydrodynamic interactions are screened, we are implicitly assuming that the small chains are effective in screening hydrodynamic interactions between monomers in the system.

In the dynamic scaling model of Rubinstein et al., the contribution of a molecule with degree of polymerization N to the complex shear modulus is given by

$$G_N^*(\omega) = \frac{d_R G_0}{2}\, i\omega \int_{\epsilon_N}^{\epsilon_x} \frac{(\epsilon/\epsilon_x)^{(d_R/2)-1}}{i\omega + \epsilon}\frac{d\epsilon}{\epsilon_x} \qquad (6)$$

where G_0 is the unrelaxed shear modulus due to the molecule, ϵ_N is the slow rate cutoff associated with the overall mass of the polymer N, ϵ_x is the high rate cutoff associated with the spacer length between branch points N_x and d_R is the dimension of the relaxation rate spectrum. Assuming a Rouse model for the polymer chains, Rubinstein et al. found

$$d_R = \frac{2d_f}{2 + d_f} \qquad (7)$$

and $\epsilon_N/\epsilon_x = (N/N_x)^{-2/d_R}$. This result for d_R has also been implicitly obtained by Cates,[28] Muthukumar,[29] and Martin et al.[30] Note that relaxation modes on frequency scales greater than ϵ_x are not included in this model, so that we should have $G_0 = \rho kT/N_x$, where ρ is the number density of monomers. The full complex modulus of the system is obtained by summing the response of each molecule from eq 6 over the distribution of molecular weights, that is

$$G^*(\omega) = \int_0^\infty n(N) N G_N^*(\omega)\, dN \qquad (8)$$

Assuming the simple double step function, eq 3 for the cutoff function gives[27]

$$G^*(\omega) = \frac{d_R G_0}{2}\frac{i\omega}{1 - (N_x/N_{char})^{\tau-2}} \times \left[\int_{\epsilon_{char}}^{\epsilon_x} \frac{(\epsilon/\epsilon_x)^{d_R(\tau-1)/2-1}}{i\omega + \epsilon}\frac{d\epsilon}{\epsilon_x} - \left(\frac{N_x}{N_{char}}\right)^{\tau-2} \int_{\epsilon_{char}}^{\epsilon_x} \frac{(\epsilon/\epsilon_x)^{(d_R/2)-1}}{i\omega + \epsilon}\frac{d\epsilon}{\epsilon_x}\right] \qquad (9)$$

where $\epsilon_{char}/\epsilon_x = (N_{char}/N_x)^{-2/d_R}$. Since $\tau < 2$ in our system, in the limit $N_{char} \gg N_x$, the second term inside the square brackets in eq 9 dominates and $G^*(\omega)$ has the limiting behavior

$$G^*(\omega) = \frac{d_R G_0}{2}\, i\omega \int_{\epsilon_{char}}^{\epsilon_x} \frac{(\epsilon/\epsilon_x)^{(d_R/2)-1}}{i\omega + \epsilon}\frac{d\epsilon}{\epsilon_x} \qquad (10)$$

that is, the complex modulus of the system is independent of the polydispersity exponent τ and is dominated by polymers with the largest characteristic degree of polymerization. Note this is qualitatively different from the limiting behavior of $G^*(\omega)$ for polymer gels where $\tau > 2$.[27] In practice, for the values of N_{char} studied in this paper, the first term inside the square brackets in eq 9 is nonnegligible and needs to be included in our modeling.

Using the exponential cutoff function eq 2 in eq 8 gives

$$G^*(\omega) = \frac{d_f}{d_f + 2}\frac{G_o}{\Gamma(2-\tau, a)} \int_0^{\epsilon_x} \frac{i\omega(\epsilon/\epsilon_x)^{(d_R/2)-1}}{i\omega + \epsilon} \Gamma\left[2 - \tau, a\left(\frac{\epsilon}{\epsilon_x}\right)^{-d_R/2}\right]\frac{d\epsilon}{\epsilon_x} \qquad (11)$$

Assuming we fix d_f (via the hyperscaling relation eq 5), eqs 9 and 11 contain two fitting parameters, which we choose to be G_0 and ϵ_x.

3. Experimental Section

3.1. Synthesis. Detailed description of the monomer synthesis can be found in Parker[3,31] and Keeney.[32] The AB_2 monomers used in our study consist of a series of dimethyl 5-(ω-hydroxyalkoxy)isophthalates of various alkyl chain lengths n ($2 \rightarrow 4$) (see Figure 1). The AB_2 monomers underwent step growth polmerization, eliminating methanol, on heating between 210 and 240 °C in a stream of dry nitrogen and in the presence of a transesterification catalyst. The catalyst is a combination of manganese(II) acetate ($Mn(OAc)_2$) and antimony trioxide (Sb_2O_3), with triphenyl phosphate ($(PhO)_3PO$) as a suppressant of thermal degradation. The resulting polymers were easily soluble in common organic solvents such as tetrahydrofuran and chloroform.

3.2. Characterization. Size exclusion chromatography (SEC) measurements were performed at 30 °C in THF. The column set consisted of three 7.5 mm diameter × 300 mm long, 5 μm particle diameter mixed-C polystyrene−divinyl benzene gel columns (pore sizes of 10^2, 10^3 and 10^5Å; Polymer Laboratories, Shropshire, U.K.). The flow rate was 1.0 mL/min with sample concentrations in the range 1.03 mg/mL (lowest molar mass) to 3.24 mg/mL (highest molar mass). A Viscotek differential refractometer/viscometer model 200 and a Viscotek right angle laser light scattering (RALLS) detector LD600 (λ_o = 670 nm) were used in conjunction with SEC. The specific refractive index increment dn/dc, determined using a Brice-Phoenix Differential refractometer varied from 0.141 mL/g (lowest molar mass) to 0.144 mL/g (highest molar mass).

Evidence of cyclization was found in these systems from MALDI−TOF mass spectrometry (see the papers by Feast et

Table 1. Properties of the Hyperbranched Polymers Studied

material	n	M_o	M_w	PDI	T_g(°C)
H30_2	2	254	30 400	3.9	82
H93_2	2	254	93 100	9.9	85
H68_3	3	268	68 300	6.2	66
H120_4	4	282	120 000	11.9	49

al.[24] and Parker and Feast[3]). The thermal properties were analyzed by differential scanning calorimetry (DSC). All the samples showed a single glass transition with no evidence of melting or crystallization peaks, indicating that the samples are amorphous.

The characteristic details of the polymers are shown in Table 1. The samples are identified by their weight-average molecular weight and the spacer length n; thus for H68_3, $M_w \approx 68 \times 10^3$ and $n = 3$ (corresponding monomer molecular weight, $M_o = 268$).

3.3. Rheology. Small amplitude oscillatory shear experiments were carried out in the linear viscoelastic regime on a Rheometrics ARES, controlled strain rheometer using a 10 mm parallel plate geometry. The thickness of the samples varied from about 0.5 to 2.0 mm. Experiments were performed under a dry nitrogen atmosphere. Frequency sweeps in the linear viscoelastic regime were performed from 0.1 to 100 rad/s within the temperature range 52.5−140 °C. The resulting frequency sweeps were time−temperature shifted to obtain mastercurves spanning many decades of frequency. Moisture did not influence the rheological measurements because the polyester samples are amorphous, and hence, we did not have to carry out measurements at high temperatures. We confirmed this by drying the samples under different conditions and found our rheological results to be independent of drying conditions.

4. Results and Discussion

4.1. Size Exclusion Chromatography. If it is assumed that each elution volume V_i corresponds to a single molar mass, the number density of molecules $n(M_i)$ of molecular weight M_i is given by[33,34]

$$n(M_i) \alpha - \frac{1}{(M_i)^2} \frac{c_i}{c} \frac{dV}{d(\log(M_i))} \tag{12}$$

where c is the area under the differential refractive index (DRI) chromatogram, and c_i/c is the weight fraction of polymer in the ith retention volume. (In fact $n(M_i)$ calculated from eq 12 is not exactly equal to the number density of molecular weight M_i because SEC separates molecules according to hydrodynamic volume rather than molecular weight. Molecules with different molecular structures and different molecular weights may have the same hydrodynamic volume.[35,36] However as we shall see later, our rheological results show that $n(M_i)$ calculated from eq 12 is a good approximation to the true molecular weight distribution for our system.) For all our samples, $\log(M_i)$ vs V was found to be linear to a good approximation (see Figure 2), that is, the derivative $dV/d(\log(M_i))$ was a constant independent of M_i (though the value of this constant varies from sample to sample). Therefore, to a good approximation, we can assume

$$n(M_i) \propto \frac{c_i}{M_i^2} \tag{13}$$

We assume a form for the number density given by eq 1 using a simple exponential cutoff for f, that is

$$n(M) \sim M^{-\tau} \exp(-M/M_{char}) \tag{14}$$

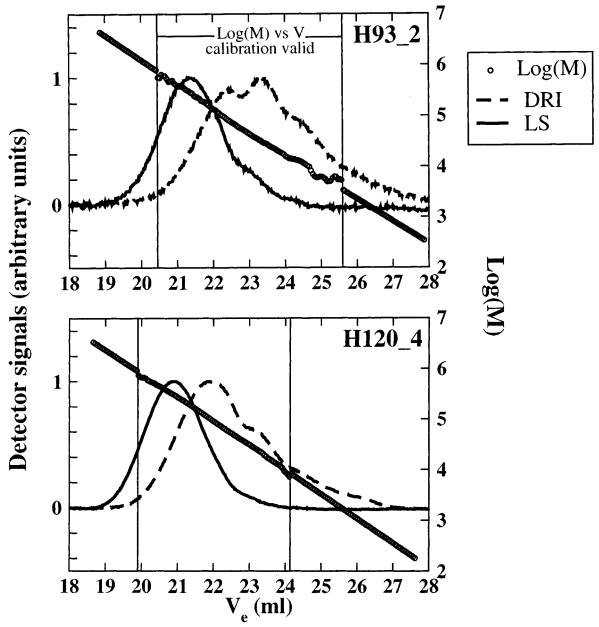

Figure 2. Validity of $\log(M)$ vs V_e data. The representative plots are for H93_2 and H120_4.

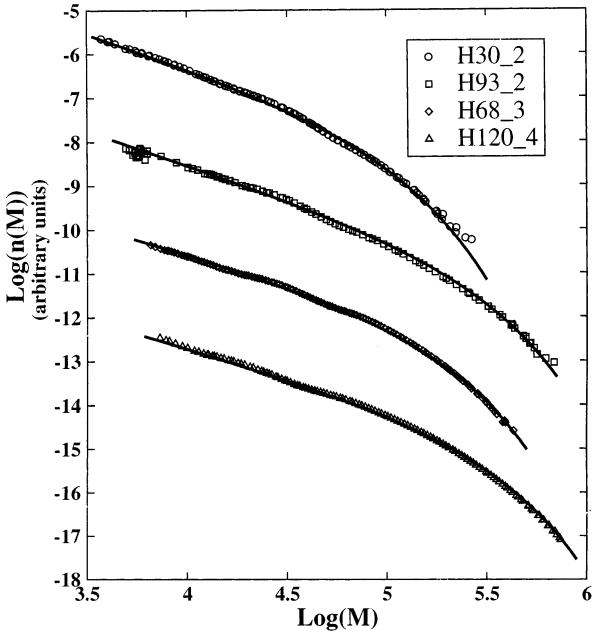

Figure 3. Molar mass distribution obtained from SEC in combination with a light-scattering detector. The data have been vertically shifted for clarity. The solid lines are two-parameter fits using eq 14.

which allows us to obtain an estimate for the exponent τ and largest characteristic molecular weight M_{char}. The tails of the molecular weight distribution measured by SEC are uncertain because of low signals in either the light-scattering or refractive index detectors. This uncertainty is evidenced by the SEC system adopting extrapolated log M vs V curves in this regime because of nonphysical measured values for M (see Figure 2; the calculation of M_i relies on a knowledge of *both* the light-scattering and refractive index signals). Because of this, in fitting the SEC data using eq 14, we have not used the low signal region of the molecular weight distribution. Figure 3 shows the two-parameter fitting to the molecular weight distribution for all the samples. Equation 14 works remarkably well for all our samples,

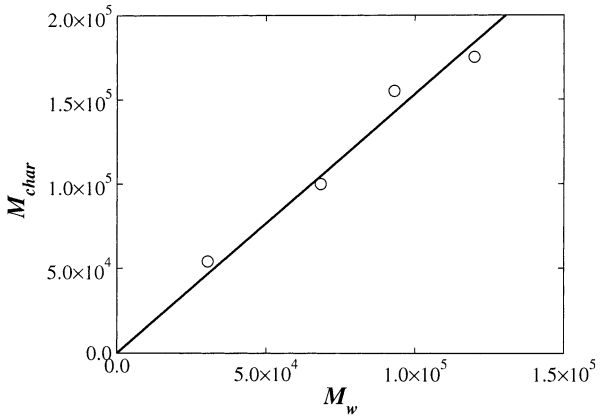

Figure 4. Characteristic molecular weight M_{char} against weight-average molecular weight M_w. $M_{char} \propto M_w$ as expected for $\tau < 2$. The solid line represents the best fit to the data through the origin.

Table 2. Static Scaling and Mark−Houwink Parameters

material	t	M_{char}	log(K)	a
H30_2	1.55	54 000	−2.056	0.22
H93_2	1.55	155 000	−2.058	0.215
H68_3	1.35	100 000	−2.41	0.32
H120_4	1.35	175 000	−2.22	0.315

justifying our static scaling assumption for the molecular weight distribution of hyperbranched polymers. The fitted values of M_{char} and τ, are given in Table 2. In Figure 4, we plot M_{char} against M_w given in Table 2. The results agree with the expected scaling relationship $M_{char} \propto M_w$, thus establishing that the values of M_{char} obtained are physically reasonable. Note that the M_w values in Table 1 have been calculated using the entire range of the molecular weight distribution, however we have checked that its value is not significantly affected by the data at the wings of the distribution (removing the data at the wings leads to a change in M_w of 5−10%); M_z on the other hand is significantly affected by the data at the higher molar mass end, but fortunately M_z is irrelevant to our discussion because $\tau < 2$ for our system (see discussion in subsection 2.1). The value of τ appears to be dependent on the alkyl chain length n of the material, so that for $n = 2$ we obtain $\tau = 1.55$ while for $n = 3$, 4 we obtain $\tau = 1.35$. These values of τ are close to but not exactly the same as the mean field value $\tau = 1.5$. This is presumably because our polymer samples were synthesized under non-mean-field polycondensation conditions, as evidenced by the presence of cycles in these materials.[24] In the limit $n \gg 1$, we expect to recover the mean-field value for τ.[37]

In Figure 5, we present Mark−Houwink plots for all our samples. The intrinsic viscosity for all our samples obey the scaling $[\eta] = KM^{\alpha}$ with $\alpha \approx 0.2 \rightarrow 0.3$; specific values are given in Table 2. Using the scaling relation for the intrinsic viscosity with molecular weight $[\eta] \propto M^{(3/d_{fs})-1}$, we deduce the fractal dimension of these hyperbranched polymers in THF (which is a good solvent for our hyperbranched polymers) to be $d_{fs} = 2.3 \rightarrow 2.5$.

4.2. Linear Rheology. The dynamic modulli (i.e., G' and G'') for all our samples are shown in Figure 6. The data have been shifted to $T_g + 20$ °C. This approximately superposes the high-frequency crossover in G' and G'' for all our samples. In the high-frequency region, the time−temperature superposition breaks down. This is especially clear looking at the dispersion in tan δ data

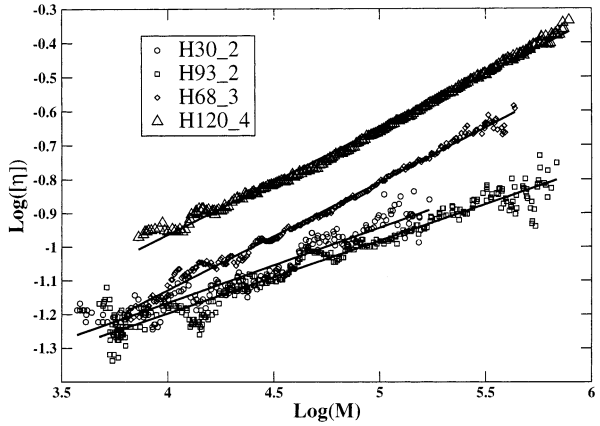

Figure 5. Mark−Houwink plots. The solid lines represent fits to the data.

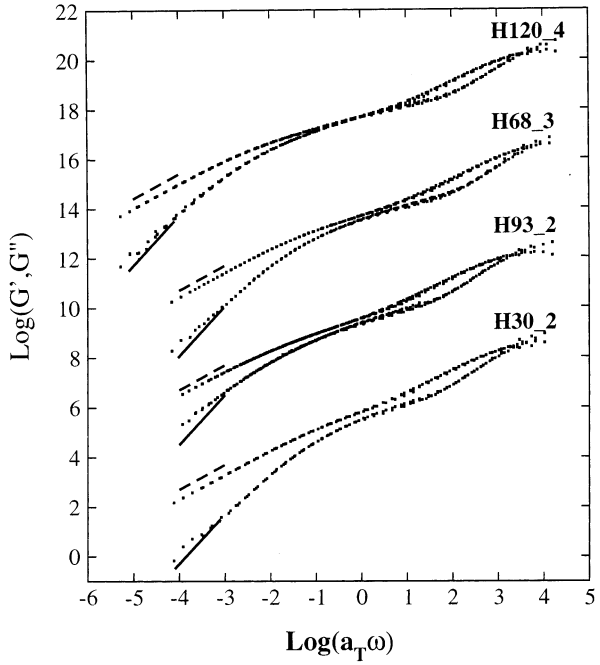

Figure 6. Master curves of dynamic modulli for all the samples. The data sets have been vertically shifted for clarity. The shift factors are 1, 10^4, 10^8, and 10^{12} for H30_2, H93_2, H68_3, and H120_4, respectively. The solid lines have a slope of 2, and the dashed lines have a slope of 1.

(see Figure 8). We therefore consider this high-frequency region as being due to glassy modes. In this paper, as we are primarily interested in modeling the low- and intermediate-frequency behavior, we shall not consider these glassy modes any further.

In the low-frequency region, for G'', we observe classical terminal scaling for H30_2, H68_3, and H120_4, that is, $G'' \sim \omega$, and close to terminal scaling for H93_2, that is, $G'' \sim \omega^{0.94}$. However for G', we observe deviations from terminal scaling for all samples, that is, for H30_2, H68_3, and H120_4 we have $G' \sim \omega^{1.6}$ while for H93_2, we have $G' \sim \omega^{1.32}$. We note that other rheological studies of dendritic polymers have also observed nonterminal G' scaling.[9,11,15,38] within the frequency range of conventional rheomtery. This indicates that this class of materials contain very slow relaxation modes. As we shall see later, for our systems, these slow relaxation modes are due to the ultrahigh molecular weight species in the exponential tail of the molecular weight distribution.

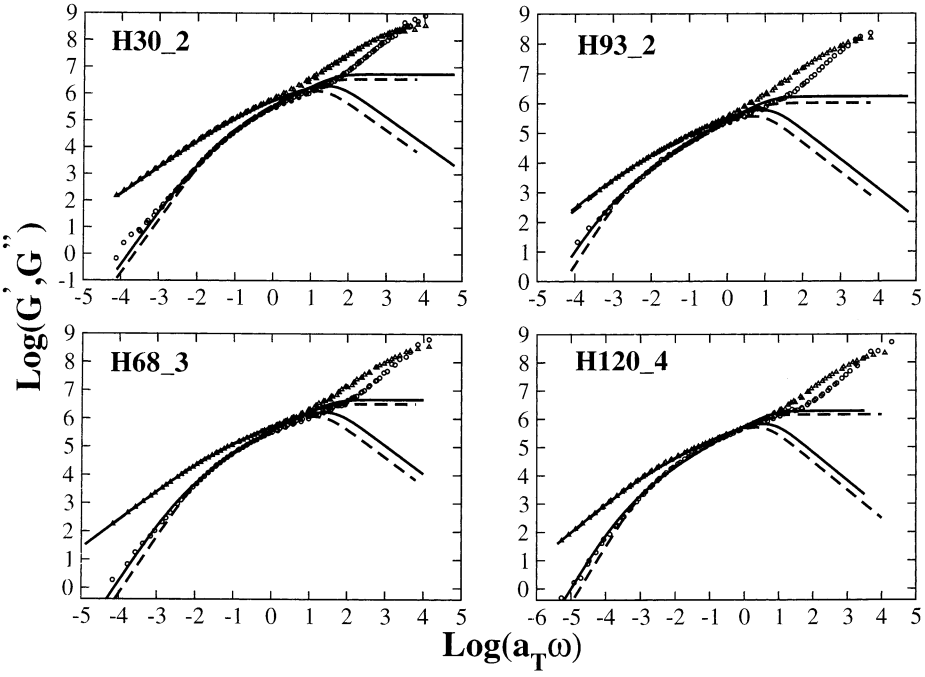

Figure 7. Storage and loss modulus against frequency for all samples for a fractal dimension of 3.0. Symbols represent the experimental data points. Dashed lines are predictions using the simple double step cutoff function whereas solid lines are predictions using the exponential cutoff function.

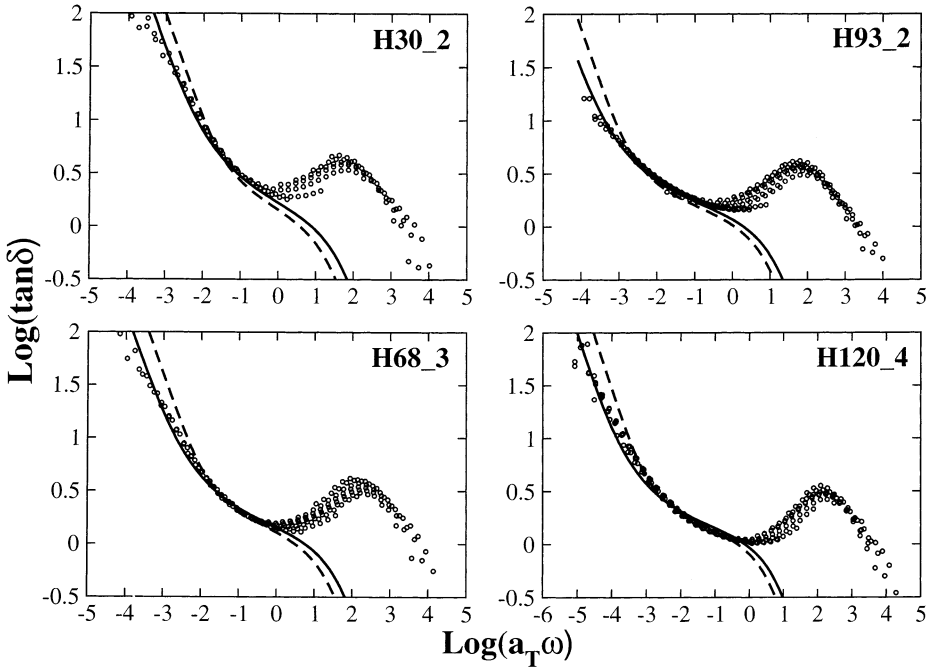

Figure 8. Plot of tan δ against frequency for all samples for a fractal dimension of 3.0. The symbols are the experimental data points. Dashed lines are predictions using the simple double step cutoff function whereas solid lines are predictions using the exponential cutoff function.

At intermediate frequencies, all the samples exhibit a scaling regime, where G', $G'' \sim \omega^{\alpha}$ over a limited frequency range. This is especially clear for the highest molecular weight sample H120_4, where the scaling regime spans up to 3 decades in frequency. This scaling regime is similar to that observed in near-critical gels[39,40] and microgels[41] and provides the motivation for applying the dynamic scaling theory in subsection 2.2 to our system. We note that for all the hyperbranched polymers, there is no crossover in G' and G'' at frequencies just above the terminal zone, unlike the case of entangled polymer systems. This suggests that entanglements are absent from our system.

In Figures 7 and 8, we show fits to the dynamic modulli and tan δ respectively using the Rouse model described in subsection 2.2, for both the simple (eq 9) and exponential cutoff functions (eq 11) with ϵ_x and G_0 as our fitting parameters and assuming $d_f = 3$ (hyperscaling relation) and $M_x = 2M_o$ (from the fact that the degree of branching is $\approx$0.5 for these samples[3,31,32]). The values of the fitting parameters are shown in Table 3. The magnitude of G_o is about the same order of

Table 3. Rheological Parameters

	simple double step cutoff		exponential cutoff	
material	ϵ_x (s^{-1})	G_o ($\times 10^6$ Pa)	ϵ_x (s^{-1})	G_o ($\times 10^6$ Pa)
H30_2	30	4.0	60	6.2
H93_2	12	1.1	20	1.8
H68_3	32.5	3.5	60	5.0
H120_4	5.5	1.5	9.0	2.0

magnitude as RT/M_x ($\approx$6.14 $\times$ 10^6, 6.19 $\times$ 10^6, 5.57 $\times$ 10^6, and 5.04 $\times$ 10^6 Pa for H30_2, H93_2, H68_3, and H120_4, respectively) and hence is in good agreement with the predictions of rubber elasticity theory. We see that while the dynamic scaling model using both the step function and exponential cutoff models the intermediate-frequency data accurately, the low-frequency data, specifically, the nonterminal scaling of G', is only modeled accurately if we use the exponential cutoff function. This shows conclusively that the nonterminal scaling in G' is due to the ultrahigh molecular weight species in the exponential tail of the molecular weight distribution. The remarkably good fits using the dynamic scaling model with exponential cutoff shows that these hyperbranched polymers can be considered to be polymeric fractals which are unentangled. It also confirms that the molecular weight distribution measured by SEC is a good approximation to the true molecular weight distribution (see discussion in section 4.1). Note that the rheological response at high frequencies is not predicted well because relaxation modes with $\epsilon > \epsilon_x$ have been neglected in the dynamic scaling model.

Up to this point, we have assumed a fractal dimension $d_f = 3$ for all our samples. It is interesting to ask how sensitive the dynamic scaling model is to variations in d_f and whether it is possible to distinguish between different values of d_f using the rheological data. From eq 9, we note that in the limit $N_{char} \gg N_x$, the dynamic modulli has the limiting behavior $G^*(\omega) \sim (i\omega)^{d_R/2}$ at intermediate frequencies $\epsilon_{char} \ll \omega \ll \epsilon_x$, where $d_R/2 = d_f/(d_f + 2)$. In principle, therefore one could determine d_f from the slope of the dynamic modulli at intermediate frequencies. In practice, for our materials, the values for N_{char} and the frequency range of the scaling regime are not large enough for d_f to be determined accurately in this way. To see if it is possible to distinguish d_f from the rheological data, we therefore perform model fits to the data over the entire frequency range.

In Figure 9, we show the best fits to the dynamic modulli G' and G'' for H120_4, for $d_f = 2$, 3, and 4. Clearly it is difficult to distinguish between the different fractal dimensions from the rheological data at low and intermediate frequencies, indicating that rheology is not very sensitive to d_f; this is probably due to the relatively narrow frequency range of the scaling regime in these systems. However, it is at least possible to say that the rheological data is consistent with the postulated hyperscaling relation $d_f = 3$. This value for the melt d_f is also consistent with the swollen fractal dimension in good solvent $d_{fs} = 2.3 \rightarrow 2.5$ obtained from the Mark–Houwink plot: physically we require $d_f > d_{fs}$ because polymers must be more swollen in good solvent than in the melt. For the future, it would be interesting to perform direct scattering studies to verify the unusual hyperscaling result $d_f = d$ for hyperbranched systems.

5. Conclusions

In this paper, we have studied the melt rheology and molecular weight distribution of four short chain branched hyperbranched polyesters with different molecular weights and containing branched monomers of various alkyl chain lengths n ($2 \rightarrow 4$). We find that the molecular weight distribution for all our samples obeys the static scaling form $n(M) \sim M^{-\tau}\exp(-M/M_{char})$. The values of the polydispersity exponent τ for all our samples (either 1.35 or 1.55) are close to but not the same as the mean field value of $\tau = 1.5$, a consequence of the fact that our polymer samples were synthesized under non-mean-field polycondensation conditions. We found that the rheology at low and intermediate frequencies could be modeled accurately using a dynamic scaling theory based on the Rouse model. This confirms that these hyperbranched polymers behave as polymeric fractals which are unentangled. This also confirms that the molecular weight distribution determined from SEC is a good approximation to the true molecular weight distribution for our materials. For these polymers, the fractal dimension in the melt was found to be consistent with the hyperscaling relation for hyperbranched polymers $d_f = 3$, although we found rheology to be rather insensitive to d_f. The fractal dimension $d_f = 3$ is also consistent with the swollen fractal dimension $d_{fs} = 2.3 \rightarrow 2.5$ determined from intrinsic viscosity measurements (physically, we require $d_f > d_{fs}$).

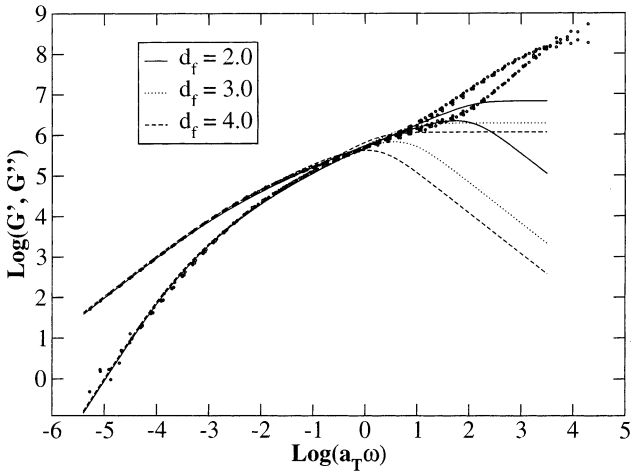

Figure 9. Predictions using the exponential cutoff function for G' and G'' for H120_3 for various fractal dimensions. Symbols represent experimental data points, and the lines are the model fits.

Acknowledgment. S. thanks the IRC for financial support in the form of a Studentship. D.M.A.B. also thanks the EPSRC for financial support in the form of an Advanced Research Fellowship.

Appendix: Derivation of the Hyperscaling Relation for Hyperbranched Polymers

In this appendix, we briefly outline the derivation of the hyperscaling relation for hyperbranched polymers given by eq 5. We hope to present a more detailed derivation soon in a future publication.[37] Our derivation essentially follows the work of Cates[26] and centers on analyzing the overlap function $\Phi(N)$ which is given by

$$\Phi(N) = \frac{R(N)^d}{N} \int_N^{N_{char}} n(N')\, N'\, dN' \qquad (15)$$

Here d (=3) is the dimension of space, $n(N)$ is the number of polymers with degree of polymerization N per lattice site given by eqs 1–3 and $R(N) \sim N^{1/d_f}$ is the

radius of gyration for a polymer (or section of a polymer) with degree of polymerization N (note that we are working in units of length where the lattice step length is 1). The overlap function $\Phi(N)$ is equal to the total hard sphere volume fraction occupied by chains of mass N and sections of larger chains of mass N. Physically, if $\Phi(N) \gg 1$, polymer chains are strongly overlapped on the mass scale of N so that the excluded volume interaction is strongly screened on that mass scale; conversely, if $\Phi(N) \ll 1$, polymer chains are not overlapped on the mass scale of N and the excluded volume interaction is not screened on that mass scale.

For hyperbranched polymers, we have $1 < \tau < 2$. Since we are interested in the limit $N_{\mathrm{char}} \gg 1$, the cutoff function given by eqs 3 and 2 can be approximated by $f \approx N_{\mathrm{char}}{}^{\tau-2}$ (for $N_x < N < N_{\mathrm{char}}$). In addition, the integral in eq 15 is dominated by the upper mass cutoff (cf. critical gels where $2 < \tau < 3$ and the integral is dominated by the lower cutoff). This means that $\int_N^{N_{\mathrm{char}}} n(N')N'\,\mathrm{d}N' \approx 1$, so that for hyperbranched polymers, the overlap function simplifies to

$$\Phi(N) \approx N^{d/d_{\mathrm{f}}-1} \tag{16}$$

For the derivation of the hyperscaling relation, we will also require d_{fg} and d_{fs}, the fractal dimension for hyperbranched polymers when the excluded volume interaction is screened and unscreened, respectively. It is possible to show[37] that $d_{\mathrm{fg}} = 4$, while at the level of Flory theory $d_{\mathrm{fs}} = 2(d + 2)/5$, that is, $d_{\mathrm{fs}} = 2$ for $d = 3$ (experimentally, we find $d_{\mathrm{fs}} = 2.3 \rightarrow 2.5$ for our hyperbranched polymers).

The true value of d_{f} for hyperbranched polymer melts can now be calculated from the following ingenious argument due to Cates. For simplicity, we specialize in the case $d = 3$. If we first assume that the excluded volume interaction for chains (or sections of chains) of mass N is screened, then $d_{\mathrm{f}} = d_{\mathrm{fg}}$, and we have $d/d_{\mathrm{fg}} - 1 < 0$. However, from eq 15, this means that $\Phi(N) \ll 1$ (for large enough N); that is, the chains are not overlapped and the excluded volume is not screened. This is clearly a contradiction. Conversely, if we assume that the excluded volume interaction for chains (or sections of chains) of mass N is unscreened, then $d_{\mathrm{f}} = d_{\mathrm{fs}}$, and (using either the Flory or experimental value for d_{fs}) we have $d/d_{\mathrm{fs}} - 1 > 0$. However, from eq 15, this means that $\Phi(N) \gg 1$ (for large enough N), that is, the chains are strongly overlapped and the excluded volume is screened. This is again a contradiction. The only way for the system to resolve this overlap paradox is for d_{f} to change so that polymer chains are marginally overlapped on all scales, that is, $\Phi(N) \approx 1$ for all N.

For hyperbranched polymers, where the overlap function is given by eq 15, this means that $d_{\mathrm{f}} = d$. For critical gels (where $2 < \tau < 3$), going through exactly the same arguments yields the more familiar hyperscaling relation $d_{\mathrm{f}} = d/(\tau - 1)$.[26] More generally, assuming the Flory value for d_{fs}, one can show that the hyperscaling relation for hyperbranched polymers given by eq 5 holds for $d = 2, 3, 4$.

References and Notes

(1) Hult, A.; Johansson, M.; Malmström, E. *Adv. Polym. Sci.* **1999**, *143*, 1−34.
(2) Jikei, M.; Kakimoto, M. *Prog. Polym. Sci.* **2001**, *26*, 1233−1285.
(3) Parker, D.; Feast, W. J. *Macromolecules* **2001**, *34*, 5792−5798.
(4) Böhme, F.; Clausnitzer, C.; Gruber, F.; Grutke, S.; Huber, T.; Pötschke, P.; Voit, B. *High Perform. Polym.* **2001**, *13*, S21−S31.
(5) Hong, Y.; Cooper-White, J. J.; Mackay, M. E.; Hawker, C.; J.; Malmström, E.; Rehnberg, N. *J. Rheol.* **1999**, *43*, 781−793.
(6) Hong, Y.; Coombs, S. J.; Cooper-White, J. J.; Mackay, M. E.; Hawker, C. J.; Malmström, E.; Rehnberg, N. *Polymer* **2000**, *41*, 7705−7713.
(7) Schmaljohann, D.; Pötschke, P.; Hässler, R.; Voit, B. I.; Frolehling, P. E.; Mostert, B.; Loontjens, J. A. *Macromolecules* **1999**, *32*, 6333−6339.
(8) Hempenius, M. A.; Zoeteleif, W. F.; Gauthier, M.; Möller, M. *Macromolecules* **1998**, *31*, 2299−2304.
(9) Simon, P. F. W.; Müller, A. H. E.; Pakula, T. *Macromolecules* **2001**, *34*, 1677−1684.
(10) Robertson, C. G.; Roland, C. M.; Paulo, C.; Puskas, J. E. *J. Rheol.* **2001**, *45*, 759−772.
(11) Kharchenko, S. B.; Kannan, R. M.; Cernohous, J. J.; Venkataramani, S.; Babu, G. N. *J. Polym. Sci. B* **2001**, *39*, 2562−2571.
(12) Namba, S.; Tsukahara, Y.; Kaeriyama, K.; Okamoto, K.; Takahashi, M. *Macromolecules* **2001**, *34*, 2624−2629.
(13) Ahn, D. U.; Kwak, S. *Macromol. Mater. Eng.* **2001**, *286*, 17−25.
(14) Kwak, S.; Ahn, D. U. *Macromolecules* **2000**, *33*, 7557−7563.
(15) Uppuluri, S.; Morrison, F. A.; Dvornic, P. R. *Macromolecules* **2000**, *33*, 2551−2560.
(16) Sendijarevic, I.; McHugh, A. J. *Macromolecules* **2000**, *33*, 590−596.
(17) Hawker, C. J.; J, F. P.; Mackay, M. E.; Wooley, K. L.; Frechet, J. M. J. *J. Am. Chem. Soc.* **1995**, *117*, 4409−4410.
(18) Flory, P. J. *J. Am. Chem. Soc.* **1952**, *74*, 2718−2723.
(19) Flory, P. J. *Principles of Polymer Chemistry;* Cornell University Press: Ithaca, NY, 1953.
(20) Müller, A. H. E.; Yan, D.; Wulkow, M. *Macromolecules* **1997**, *30*, 7015−7023.
(21) Yan, D.; Müller, A. H. E.; Matyjaszewski, K. *Macromolecules* **1997**, *30*, 7024−7033.
(22) Yan, D.; Zhou, Z.; Müller, A. H. E. *Macromolecules* **1999**, *32*, 245−250.
(23) Zhou, Z.; Yan, D. *Polymer* **2000**, *41*, 4549−4558.
(24) Feast, W. J.; Keeney, A. J.; Kenwright, A. J.; Parker, D. *Chem. Commn.* **1997**, 1749.
(25) Stauffer, D.; Aharony, A. *Introduction to Percolation Theory*, revised 2nd ed.; Taylor & Francis: London, 1994.
(26) Cates, M. E. *J. Phys., Lett.* **1985**, *46*, 837−843.
(27) Rubinstein, M.; Colby, R. H.; Gillmor, J. R. In *Space-Time Organisation in Macromolecular Fluids*; Tanaka, F., Doi, M., Ohta, T., Eds.; Springer-Verlag: Heidelberg, Germany, 1989.
(28) Cates, M. E. *J. Phys. (Paris)* **1985**, *46*, 1059−1077.
(29) Muthukumar, M. *J. Chem. Phys.* **1985**, *83*, 3161−3168.
(30) Martin, J. E.; Adolf, D.; Wilcoxon, J. P. *Phys. Rev. Lett.* **1988**, *61*, 2620−2623.
(31) Parker, D. Ph.D. thesis, University of Durham, 2000.
(32) Keeney, A. J. Ph.D. thesis, University of Durham, 1998.
(33) Lusignan, C. P.; Mourey, T. H.; Wilson, J. C.; Colby, R. H. *Phys. Rev. E* **1999**, *60*, 5657−5669.
(34) Lusignan, C. P. Ph.D. thesis, University of Rochester, 1996.
(35) Leibler, L.; Schossler, F. *Phys. Rev. Lett.* **1985**, *55*, 1110−1113.
(36) Schossler, F.; Benoit, B.; Grubisic-Gallot, Z.; Strazielle, C.; Leibler, L. *Macromolecules* **1989**, *22*, 400−410.
(37) Buzza, D. M. A. Submitted to Europhys. Lett.
(38) Jahromi, S.; Palmen, J. H. M.; Steeman, P. A. M. *Macromolecules* **2000**, *33*, 577−581.
(39) Chambon, F.; Pertrovic, Z. S.; MacKnight, W. J.; Winter, H. H. *Macromolecules* **1986**, *19*, 2146−2149.
(40) Nicolai, T.; Randrianantoandro, H.; Prochazka, F.; Durand, D. *Macromolecules* **1997**, *30*, 5897−5904.
(41) Antoneitti, M.; Rosenauer, C. *Macromolecules* **1991**, *24*, 3434−3442.
(42) Muthukumar, M.; Winter, H. H. *Macromolecules* **1986**, *19*, 1284−1285.
(43) Nunez, C, M.; Chiou, B.; Andrady, A. L.; Khan, S. A. *Macromolecules* **2000**, *33*, 1720−1726.
(44) Kapnistos, M.; Semenov, A. N.; Vlassapoulos, D.; Roovers, J. *J. Chem. Phys.* **1999**, *111*, 1753−1759.
(45) de Gennes, P. G. *Scaling Concepts in Polymer Physics;* Cornell University Press: Ithaca, NY, 1988.
(46) Cameron, C.; Fawcett, A. H.; Hetherngton, C. R.; Mee, R. A. W.; McBride, F. V. *Macromolecules* **2000**, *33*, 6551−6568.

MA020820R